JETIR.ORG ISSN: 2349-5162 | ESTD Year : 2014 | Monthly Issue

JOURNAL OF EMERGING TECHNOLOGIES AND INNOVATIVE RESEARCH (JETIR)

An International Scholarly Open Access, Peer-reviewed, Refereed Journal

Bitwise Channel Estimation for UL/DL For Massive MIMO

Abdul Rafay Akber[1], Mohammed Fahad[2], Ahsan[3], Dr. Abdul Mateen Ahmed[4]

Students[1,2,3], Asst professor[4]

Department of ECE[1,2,3,4]

ISL Engineering College, Hyderabad, Telengana, India

ABSTRACT

In this paper, we propose a multipath extraction-based uplink/downlink channel estimation scheme for wideband massive multiple-input multiple-output (MIMO) systems, where orthogonal frequency division multiplexing (OFDM) is adopted and the beam squint effect is considered. Firstly, we investigate the spatial- and frequency-wideband effects and obtain the relationship between angle-delay information and coordinates of on-grid paths. Secondly, according to the spatial- and frequency-wideband effects, we design a pilot pattern in uplink training to ensure that exact paths can be acquired from limited potential paths. Combined with pilot pattern design, a modified density-based spatial clustering of applications with noise (M-DBSCAN) approach is proposed to acquire the on-grid potential paths. Potential paths are used for initialization in uplink channel extraction. Due to the fact that coordinates of only a few potential paths are close to those of true paths, the uplink multipath extraction problem can be regarded as an off-grid sparse signal reconstruction problem. To deal with this issue, an off-grid sparsity adaptive matching pursuit (OSAMP) based compressive sensing method with low computational complexity is proposed. With the aid of antenna array theory and array signal processing, we build a spatial basis expansion model (SBEM) to represent the UL/DL channels with much fewer parameter dimensions. Hence, both UL and DL channel estimation of multiusers can be carried out with a small amount of training resource, which significantly reduces the training overhead and feedback cost. Simulation results are provided to demonstrate the effectiveness of our proposed low computational complexity channel estimation method.

INTRODUCTION

Large-scale multiple-input multiple-output (MIMO) or "massive MIMO" systems [1][2] have drawn considerable interest from both academia and industry. Theoretically, massive MIMO systems can almost perfectly relieve the inter-user interference in multiuser MIMO (MU-MIMO) systems with
simple linear transceivers [3]. It was shown in [4] that each antenna element of a very large MIMO system consumes exceedingly low power, and the total power can be made inversely proportional to the number of antennas. Other advantages, such as high spectral efficiency, security, robustness
or reliable linkage, also play key roles in promoting massive MIMO systems appealing for the next generation of wireless systems [4], [5].

However, all these potential gains rely heavily on the perfect channel state information (CSI) at the base station (BS). From the conventional orthogonal training strategy [6], the optimal number of training streams should be the same as the number of the transmit antennas, and the length of the training should be no less than the number of transmit antennas. Hence, downlink (DL) training in massive MIMO system requires huge number of orthogonal training sequences. This severe overhead as well as the accompanied high calculation complexity will overwhelm the system performance and mitigate any possible improvement. For uplink (UL) training, the conventional channel estimation methods are generally feasible.

However, as the number of users or the number of user's antennas grows, the increased pilot overhead will deteriorate the system efficiency and become the system bottleneck. If the non-orthogonal sequences are used, then the so-called pilot contamination will also deteriorate the system performance.

Massive multiple-input multiple-output (MIMO) wireless transmission that adopts hundreds or thousands of antennas at the base station (BS) is regarded as a promising technique for the 5-th generation (5G) and future mobile communication networks [1],[2],[3]. Massive MIMO can simultaneously serve several users in the same time-frequency resources and thus can improve spectrum efficiency, energy efficiency, spatial resolution, and network coverage [4]-[7]. Meanwhile, massive MIMO can combat high path-loss and fading [8]. As a result, it is easy to combine the high frequency transmission, e.g., millimeter-wave (mmWave) wireless transmission and terahertz wireless transmission, with massive MIMO technologies. Moreover, enhanced mobile broadband (eMBB) is a major service class of 5G and it desires bandwidth resources to achieve transmission rates for the demand of eMBB services [9], [10].

For time division duplex (TDD) massive MIMO systems, DL CSI can be obtained by leveraging the channel reciprocity [7], which has promoted quite many research works [8]–[12]. However, in practice the channel reciprocity between UL and DL may not exactly hold even for TDD systems due to the calibration error between the UL/DL radio frequency chains [13]. In addition, the property of channel reciprocity has been proven to be robust only for the single-cell scenario [14],

and this will undoubtedly increase the pressure of multi-cell coordination. On the other side, the DL channel estimation for frequency division duplex (FDD) massive MIMO system is always deemed as a difficult problem since the channel reciprocity does not hold and cannot be used to simplify the estimation. The authors of [3], [15], [16] applied the closed loop training schemes to sequentially design the optimal pilot beam patterns. The compressive sensing (CS) based feedback reduction in [17] and the distributed compressive channel estimation in [17] exploited the channel sparsity to reduce the heavy burden of feeding back large amount of measurements. Except for the above regular attempts, a new way to design the transmission strategy for massive MIMO system is to exploit the low-rank approximation of channel covariance matrix [19]–[21]. Based on the assumption that the angular spread (AS) of the incident signals at BS from each user is narrow, the authors in [19]–[21] proposed to reduce the dimensionality of the effective channels through eigen-decomposition of channel covariance matrices. All these covariance-aware methods could be categorized into spatial division multiplexing that utilizes non-overlapped spatial information of different users to realize the orthogonal transmission.

RELATED WORK

Fortunately, recent study and experiments have shown that wireless channels between the BS and users exhibit a small angle spread seen from the BS. Due to the large dimension of the channels and the small angle spread, massive MIMO channels exhibit the sparsity in the virtual angular domain [13]. In TDD, spatial-temporal sparse structures are exhibited to learn time-varying massive MIMO channels under the hybrid analog-digital architecture [14]_[16]. In FDD, by exploiting the spatial sparsity of massive MIMO channels, compressive sensing (CS) based channel estimation and feedback schemes were utilized in massive MIMO systems to reduce the downlink training overhead and the feedback overhead [13], [17]_[23]. In [13], [17]_[20], a new CSI feedback and estimation framework was introduced, where the users fed back the received pilot signals to the BS without any signal processing procedures and multi-user channels were jointly estimated at the BS. In [21], channel estimation for wideband systems was proposed and the multiple-subcarrier channels were jointly estimated under an adaptive channel estimation and feedback framework. By exploiting the spatial correlation of massive MIMO channels, feedback overhead could also be reduced [22], [23]. It is worth noting that most of the existing works that exploited angle domain sparsity for channel estimation [13], [17]_[21] were based on on-grid CS which could only obtain the estimated channels on fixed grids. That is not suitable for realistic propagation environment as the scatterers are often located in-between the quantized grid points. Thus these on-grid channel estimation methods would decrease the performance of CS based channel estimation due to the grid mismatch effects. Recently, off-grid CS methods were proposed to improve reconstruction accuracy with acceptable complexity [24]_[26]. Such off-grid algorithms were proved to provide superior performance to the on-grid ones. In massive MIMO systems, when the number of antennas equipped at the BS is large and the signal bandwidth is wide, there is a non-negligible time delay across the array aperture for the same data symbol. Such phenomenon incurs an inherent property of large size arrays, which is called spatial-wideband effect and would correspondingly cause beam squint effect in frequency-domain [28]. Spatial-wideband effect is ignored in most of the existing massive MIMO studies in which the utilized massive MIMO channel models are directly extended from the conventional MIMO channel models [28], [29]. Therefore, when we design massive MIMO systems, spatial-wideband effect should be taken into consideration, which leads to a reformulation of many fundamental issues of massive MIMO systems that use the extended conventional MIMO channel models. Authors in [27], [30]_[32] investigated channel estimation in massive MIMO systems via off-grid channel estimation methods and took beam squint effect into consideration. Full OFDM sub-carriers were used for channel estimation in [27], [32] while comb-type pilots are utilized in [30], [31]. The parameter estimation accuracy was limited in [27] as different paths would interfere with each other. The parameter estimation accuracy was improved in [32] via an iterative reweighted approach by utilizing the shift-invariant block sparsity. However, this iterative reweighted approach was computational complex, especially in delay estimation. What's worse, it still did not guarantee a monotonically decreasing objective function value and thus the algorithms were very likely to be trapped in undesired local minima [33], which degraded the channel estimation performance. In [30], a parameterized model was applied to obtain accurate angle and delay information for channel reconstruction, where an extended relevance vector machine based sparse prior model was introduced and Newton's method was adopted at a large computing over-head. Extending from [30], authors in [31] investigated the channel estimation problem in multi-user mmWave massive MIMO-OFDM systems. With estimated channel parameters, user grouping and hybrid precoding were also investigated in [31]. In [30]_[32], based on estimated angle and delay

information, downlink precoder was designed for pilot transmission to estimate downlink channel path gains. However, the channel asymptotic orthogonal property used for down-link precoder design still caused a degradation in downlink path gain estimation, which was blamed for the decrease of downlink channel estimation performance. Besides, the computational complexity of the algorithms in [30]_[32] limited the expansion to scenarios with larger number of antennas at the BS and wider bandwidth for signal transmission.

More-over, a relatively large number of possible paths should be set for initialization, which further increased the burden of computation. Unfortunately, in the initialization of existing uplink channel extraction algorithms, the acquisition of a few qualified potential paths has not been studied.

SYSTEM MODEL

A. MASSIVE MIMO UPLINK CHANNEL MODEL

In this section, we introduce the wideband channel model. We consider that the BS equipped with a uniform linear array (ULA) of *M* antennas serves several single-antenna users. Denote *fs* as the transmission bandwidth, *N* as the number of OFDM subcarriers, *f*0 D *fs*/*N* as the frequency spacing, *fc* as the uplink carrier frequency, _*c* as the corresponding wavelength and *d* as the antenna spacing. For a certain user, we assume that there are *L* incident paths from the user side to the BS. Denote _*l*;*m* as the time delay of the *l*-th path from the user side to the *m*-th antenna of the BS and denote _*l* 1D _*l*;1 for notational simplicity, where *l* 2 f1; _ _ _ ; *L*g, *m* 2 f1; _ _ _ ;*M*g. Denote #*l* as the direction of arrival (DoA) of the *l*-th path and define '*l* D *d* sin #*l*=_*c* as the normalized DoA. We assume that the distance between the BS station and the scatterers around it is much greater than the array aperture, then based on the far-field assumption [33] shown as in Fig. 1, we have

$$\tau_{l,m} = \tau_l + (m-1)\varphi_l / f_c.$$

Denote the complex channel gain of the *l*-th path as N*l*. Then, the space-time uplink channel between the user side and the *m*-th antenna at the BS can be expressed as

$$h_m^{ST} = \sum_{l=1}^{L} \bar{\beta}_l e^{-j2\pi f_c \tau_{l,m}} \delta(t-\tau_{l,m}) = \sum_{l=1}^{L} \beta_l e^{-j2\pi(m-1)\varphi_l} \delta(t-\tau_{l,m}),$$

Where $\beta_l \triangleq \bar{\beta}_l e^{-j2\pi f_c \tau_l}$ is the equivalent complex gain. By taking the Fourier transform of (2), the uplink spatial-frequency response between the *m*-th antenna at the BS and the user side can be obtained as

$$h_m^{\mathrm{SF}}(f) = \sum_{l=1}^{L} \beta_l e^{-j2\pi(m-1)\varphi_l} e^{-j2\pi f \tau_{l,m}} = \sum_{l=1}^{L} \beta_l e^{-j2\pi(m-1)\varphi_l} e^{-j2\pi f \tau_l} e^{-j2\pi f(m-1)\frac{\varphi_l}{f_c}}.$$

Thus the overall uplink spatial-frequency channel vector from all *M* antennas can be formulated as

$$\mathbf{h}^{\mathrm{SF}}(f) = \sum_{l=1}^{L} \beta_l \mathbf{a}\left((1+\frac{f}{f_c})\varphi_l\right) e^{-j2\pi f \tau_l},$$

Where $\mathbf{a}(\varphi) = [1, e^{-j2\pi\varphi}, \cdots, e^{-j2\pi(M-1)\varphi}]^T$ is the spatial domain steering vector. Moreover, the overall frequency domain channel model for all *N* subcarriers can be grouped into one matrix as

$$\mathbf{H} = [\mathbf{h}^{\mathrm{SF}}(0), \mathbf{h}^{\mathrm{SF}}(f_0), \cdots, \mathbf{h}^{\mathrm{SF}}((N-1)f_0)] = \sum_{l=1}^{L} \beta_l (\mathbf{a}(\varphi_l)\mathbf{b}^T(\tau_l)) \odot |\Theta(\varphi_l),$$

Where $\mathbf{b}(\tau) = [1, e^{-j2\pi f_0 \tau}, \cdots, e^{-j2\pi(N-1)f_0\tau}]^T$ can be viewed as the frequency domain steering vector pointing towards delay, 2('*l*) is a phase shifting matrix with the (*m*; *n*)th element

It should be noted that 2('*l*) expresses the effect of beam squint which appears to be obvious especially when a large bandwidth is used in massive MIMO systems. In 2('*l*), there exists a phase shift (*m* - 1)(*n* - 1)*f*0'*l*=*fc* and the maximum phase shift can be approximate. For a small-scale array or a large-scale array with narrow bandwidth, the maximum shift is *fs*/*fc* = *d*/_*c M*, so that the phase shift is close to zero, leading to the phase shifting matrix 2('*l*) for each path being approximate to an all-ones matrix. In this case, the beam squint effect can be ignored and the channel model in (5) is just the channel model directly extended from the conventional ones. However, for a large-scale array with large bandwidth, *fs*/*fc* = *d*/*c M* is no longer valid, the beam squint effects cannot be ignored and signal processing methods for conventional channel models do not work anymore.

PROBLEM FORMULATION

As we can see from (5), uplink CSI of different subcarriers is determined by three kinds of parameters, i.e., path gains, DoAs and delays. To estimate these three kinds of parameters, not all the subcarriers are needed for pilot transmission. Thus we assume that comb-type pilots are used for channel estimation and suppose that there are *P* subcarriers within subset P C {1; 2; _ _ _; *N*} used for pilot transmission. Moreover, we assume that the physical location of a user changes much slower than the channel variation, indicating that the angle and delay information changes much slower than channel gains. Consider that *T u* time slots are used for uplink pilot transmission. The uplink channel vector at the *t*-th (1 < *t* < *T u*) time slot on the *p*-th subcarrier which is used for pilot transmission can be denoted as

$$\mathbf{h}^u(p,t) = \sum_{l=1}^{L} \beta_l(t)\mathbf{a}\left(\left(1+\frac{(\mathcal{P}(p)-1)f_0}{f_c}\right)\varphi_l\right) e^{-j2\pi(\mathcal{P}(p)-1)f_0\tau_l},$$

the received signal on the *p*-th (1< *p* < *P*) subcarrier at the *t*-th time slot at the BS can be expressed as

$$\bar{\mathbf{y}}(p,t) = \mathbf{h}(p,t)x(p,t) + \bar{\mathbf{w}}(p,t),$$

where *x*(*p*; *t*) is the uplink transmitted pilot signal after pre-coding, **w**N (*p*; *t*) is the associated additive white Gaussian noise (AWGN) and **w**N (*p*; *t*) _ CN(0; _2 0 **I***M*). The pilot signal is set as *x*(*n*; *t*) D *ej_n*;*t* with _*n*;*t* obeying the independent identically distributed uniform distribution in [0; 2*π*]. The received signal on the *p*-th subcarrier at the *t*-th time slot at the BS can be further processed as

$$\mathbf{y}(p,t) = \bar{\mathbf{y}}(p,t)e^{-j\xi_{p,t}} = \mathbf{h}^u(p,t) + \bar{\mathbf{w}}(p,t)e^{-j\xi_{p,t}} = \mathbf{h}^u(p,t) + \mathbf{w}(p,t).$$

Then all received pilots from *P* pilot subcarriers can be formulated as

$$\mathbf{Y}(t) = \mathbf{H}^u(t) + \mathbf{W}(t),$$

where $\mathbf{Y}(t)$, $\mathbf{H}(t)$ and $\mathbf{W}(t)$ are all matrices of dimension M x P with the p-th column as $\mathbf{y}(p; t)$, $\mathbf{h}(p; t)$ and $\mathbf{w}(p; t)$, respectively. Denote

$$f(\boldsymbol{\varphi}, \boldsymbol{\tau}, \mathbf{B}) \triangleq \sum_{t=1}^{T^u} ||\mathbf{Y}(t) - \mathbf{H}^u(t)||_2^2 = \sum_{t=1}^{T^u} ||\mathbf{y}(p,t) - \sum_{l=1}^{L} \beta_l(t)\mathbf{a}\left(\left(1+\frac{(\mathcal{P}(p)-1)f_0}{f_c}\right)\varphi_l\right) e^{-j2\pi(\mathcal{P}(p)-1)f_0\tau_l}||_2^2,$$

where $\boldsymbol{\varphi} = [\varphi_1, \varphi_2, \cdots, \varphi_L]^T, \boldsymbol{\tau} = [\tau_1, \tau_2, \cdots, \tau_L]^T$, and **B** is a matrix with dimension M _ T u. The t-th column of **B** is $\boldsymbol{\beta}(t) = [\beta_1(t), \beta_2(t), \cdots, \beta_L(t)]^T$. Then, the uplink channel extraction can be formulated as an optimization problem as

$$(\hat{\boldsymbol{\varphi}}, \hat{\boldsymbol{\tau}}, \hat{\mathbf{B}}) = \arg\min_{\boldsymbol{\varphi}, \boldsymbol{\tau}, \mathbf{B}} f(\boldsymbol{\varphi}, \boldsymbol{\tau}, \mathbf{B}).$$

SPATIAL- AND FREQUENCY-WIDEBAND PROPERTY OF MULTI-SUBCARRIER CHANNELS

If comb-type pilots are used for channel estimation, conclusions drawn in [26] are not valid any more. In this section, we characterize the spatial- and frequency-wideband property of multi-subcarrier channels. The spatial-wideband property can be obtained by the left inverse discrete Fourier transform (IDFT) of channel matrix $\mathbf{H}u$, where the index t is ignored for notational simplicity due to the slow channel variation. Denote the channel matrix for the l-th path as $\mathbf{H}ul$, the IDFT of $\mathbf{H}ul$ is shown in (12), at the bottom of the page. The amplitude of the (mN ; p)-th element of the spatial-property matrix after IDFT is

$$[\mathbf{F}_M^H\mathbf{H}_l^u]_{\bar{m},p} = \frac{\beta_l}{\sqrt{M}}\sum_{m=1}^{M} e^{-j2\pi(m-1)\varphi_l} e^{-j2\pi f_0(\mathcal{P}(p)-1)\tau_l} e^{-j2\pi(m-1)(\mathcal{P}(p)-1)f_0\frac{\gamma_l}{f_c}} e^{j\frac{2\pi}{M}(m-1)(\bar{m}-1)}$$
$$= \frac{\beta_l}{\sqrt{M}} \cdot \frac{\sin(\pi M(\frac{\mathcal{P}(p)-1}{N}\cdot\frac{f_s}{f_c}\varphi_l + \varphi_l - \frac{\bar{m}-1}{M}))}{\sin(\pi(\frac{\mathcal{P}(p)-1}{N}\cdot\frac{f_s}{f_c}\varphi_l + \varphi_l - \frac{\bar{m}-1}{M}))} e^{-j\pi(M-1)(\frac{\mathcal{P}(p)-1}{N}\cdot\frac{f_s}{f_c}\varphi_l + \varphi_l - \frac{\bar{m}-1}{M})} e^{-j2\pi f_0(\mathcal{P}(p)-1)\tau_l}$$

$$|[\mathbf{F}_M^H\mathbf{H}_l^u]_{\bar{m},p}| = \frac{\beta_l}{\sqrt{M}} \cdot \frac{\sin(\pi M(\frac{\mathcal{P}(p)-1}{N}\cdot\frac{fs}{f_c}\varphi_l + \varphi_l - \frac{\bar{m}-1}{M}))}{\sin(\pi(\frac{\mathcal{P}(p)-1}{N}\cdot\frac{fs}{f_c}\varphi_l + \varphi_l - \frac{\bar{m}}{M}))}.$$

$$[\mathbf{H}_{\mathcal{P}}^u\mathbf{F}_N^*(\mathcal{P})]_{m,p} = \sum_{p=1}^{P}\beta_l e^{-j2\pi(m-1)\varphi_l} e^{-j2\pi f_0(\mathcal{P}(p)-1)\tau_l} e^{-j2\pi(m-1)(\mathcal{P}(p)-1)f_0\frac{\gamma_l}{f_c}} e^{j\frac{2\pi}{N}(\mathcal{P}(p)-1)(\bar{n}-1)}$$
$$= \frac{\beta_l}{\sqrt{N}} \cdot \frac{\sin(\pi Pr(\frac{(m-1)f_0}{f_c}\varphi_l + \tau_l f_s - \frac{\bar{n}-1}{N}))}{\sin(\pi r(\frac{(m-1)f_0}{f_c}\varphi_l + \tau_l f_s - \frac{\bar{n}-1}{N}))} e^{-j\pi(\mathcal{P}(P)-1)r(\frac{(m-1)f_0}{f_c}\varphi_l + \tau_l f_s - \frac{\bar{n}-1}{N})} e^{-j2\pi(m-1)\varphi_l}.$$

When $M \to \infty$, there is an approximation that

$$\lim_{M\to\infty} |[\mathbf{F}_M^H\mathbf{H}_l^u]_{\bar{m},p}| = \sqrt{M}\beta_l\delta\left(\left(\frac{\mathcal{P}(p)-1}{N}\cdot\frac{fs}{f_c}+1\right)\varphi_l - \frac{\bar{m}-1}{M}\right)$$

where mN is a certain index in virtual angle domain, $\mathbf{F}M$ is a DFT matrix of dimension M X M.

Before characterizing the frequency-wideband property, we assume that uniformly distributed pilot placement is adopted and the pilot value for the p-th pilot subcarrier at the t-th time slot is set as $x(p; t)$ D $ej\_p;t$. Moreover, we assume the frequency spacing of pilot subcarriers is $rf0$. Hence, for the l-th path, the frequency-wideband property which can be obtained by the right IDFT of the channel matrix $\mathbf{H}ul$ is expressed as in (17), shown at he bottom of the next page. When the number of pilot subcarriers $P \to \infty$, there is an approximation that

$$\lim_{P\to\infty} |[\mathbf{H}_l^u\mathbf{F}_N^*(\mathcal{P})]_{m,\bar{n}}| = \sqrt{\frac{P}{N}}\beta_l\delta\left(r\left(\frac{(m-1)f_0}{f_c}\varphi_l + \tau_l f_s - \frac{\bar{n}-1}{N}\right)+s\right).$$

In another word, when fixing 'ψl, for a certain m, there are r indexes of Nn corresponding to τl. Therefore, different from the relationship between 'l and index mN , no one-to-one relationship between _l and Nn exists. Besides, the spacing between adjacent supports in virtual delay domain approximates N/r.

When system parameters for uplink transmission are set as M = 512, N = 1024, P = 16, r = 7, L = 6, SNR = 20dB, an illustration of a special case of the amplitude of received processed pilot signal in angle-delay domain $\mathbf{Z}(t) = \mathbf{F}^H{}_M\mathbf{Y}(t)\mathbf{F}^*{}_N$ (P) is shown in Fig. 2. In Fig. 2, different supports correspond to different paths. Combined with the analysed spatial- and frequency-property, we can draw conclusions as follows. (a). The cluster number of supports appearing from

the row aspect is related to the number of transmission paths, and the indexes of these rows are related to the corresponding DoAs, e.g., the clusters exist in about 6 rows in Fig. 2. (b). The cluster number of supports appearing from the column aspect is related to the spacing of pilot subcarriers, e.g., in Fig. 2, for each row where supports exist, there are about 7 clusters and the spacing between any two adjacent clusters is about 1024/7. Moreover, column indexes of supports in these rows are related to both corresponding DoAs and delays.

B. PILOT PATTERN DESIGN

Note that when s is selected as 0; 1; _ _ _ ; r - 1, respectively, there are r clusters appearing in the column aspect, which makes a confusion of the relationship between s and index Nn. Thus, it is hard to directly obtain parameter ψl according to the frequency-wideband property when 'l is fixed. What's worse, when pilot subcarriers are uniformly distributed in the whole bandwidth, the corresponding support clusters appear to be N/P, e.g., we set N = 1024 and P = 16, the number of clusters is r = N/P = 64. The large number of clusters makes the acquirement of relationship between s and index Nn more confused. Additionally, paths in most of the clusters are useless for exact path acquisition which will lead to a waste of computational resources. In this sub-section, we propose a pilot pattern design scheme for the benefit of making the relationship between s and index Nn clearer.

An intuitive solution is that G_ D 2 can achieve the corresponding maximal minimal Euclidean distance. Under this circumstance, $\{r^*_g\}^2_{g=1}$ can be obtained by exhaustive search. As a result, both of values that in set S1 and S2 have the smallest Euclidean distance are $n0$ which corresponds to the situation of s = 0 and thus the relationship between s and Nn_ is obtained. Moreover, it should be noted that mod (τfs;N) can be obtained when the relationship between s and Nn is determined. However, the acquisition of the exact value of _l is difficult. Fortunately, mod(τfs;N) is enough for the reconstruction of wireless channels.

POTENTIAL PATH SELECTION

Intuitive relationship between angle-delay information and coordinates of on-grid paths can be seen from Fig. 2. However, this relationship is only established when DoAs of different paths are obviously distinguishable and pilot subcarriers are

selected as $\max(|\frac{\mathcal{P}(p)-\bar{1}}{N} \cdot \frac{fs}{f_c} M\varphi_l|) < 1$. In real scenario, DoAs of different paths may not be obviously distinguishable and $\max(|\frac{\mathcal{P}(p)-\bar{1}}{N} \cdot \frac{fs}{f_c} M\varphi_l|)$ may larger than 1 which will lead to a non-negligible spread in angle domain. Under these circumstances, using intuitive spatial-and frequency-wideband property for channel extraction will lead to interference of different paths. Thus, instead of directly figuring out true paths of the channel, we aim to present a set of potential paths, then true paths are further acquired from the potential paths.

Note that not all subcarriers are used for pilot transmission, and that different paths may have a similar DoA, thereby algorithms in [27] is not suitable any more. Moreover, algorithms in [30]_[32] rely heavily on the initial parameters, and thus a large amount of initialized potential paths are also needed for algorithms in [30]_[32] to operate, which further increased the computational complexity. Unfortunately, how to obtain the effective initialized potential paths in a few numbers has not been studied.

In this section, combined with our proposed pilot pattern, M-DBSCAN is proposed to acquire the potential paths. Firstly, we collect supports from j**Z***g*(*t*)j and pick up the common supports of different groups, where **Z***g*(*t*) D **F***H M***Y**(*t*)**F**_*N* (P*g*). The acquired common supports are viewed as the situation of *s* D 0. As angle and delay domain spreads exist, the true common supports may form 2-dimension clusters. Thus if the common supports form a cluster, it may correspond to a potential path; if the common support forms an isolated point, it can be seen as a noisy point. Secondly, we modify DBSCAN to extract more exact potential locations of true paths. M-DBSCAN is shown in Algorithm 1. In Algorithm 1, we aim to _nd peaks of each row of j**Z***g*(*t*)j when the signal amplitude is large enough and mark the row neighborhood of the peaks as potential supports in step 1. In step 2, we pick up common supports of different groups which may correspond to the situation of *s* = 0. In step 3, we calculate the number of common supports and stack the coordinates of nonzero elements. Due to the periodicity of '*l* and _*l* in angle and delay domain, some mod operations are needed in Algorithm 1 and the distance **D** of the picked common supports should be reformulated. Thus the distance **D** is calculated in a rotating way in step 4, which makes our proposed M-DBSCAN different from the traditional DBSACN scheme. Step 5-20 classify the picked common supports. In M-DBSCAN, threshold ε controls the number of potential paths that will be classified. A smaller ε enables a larger number of potential paths to be classified and thus the number of potential paths is large. On the contrary, a larger ε enables a smaller number of potential paths but it will treat some true paths as noisy points. We prefer to choose a small ε and acquire exact paths from the classified supports. Simulation results will verify the effectiveness of M-DBSCAN.

Algorithm 1 M-DBSCAN

Require: Signals $\mathbf{Z}_g(t)$, $g = 1, 2, t = 1, \cdots, T^u$.

Ensure: $\bar{\mathbf{Z}}_g = \mathbf{0}, g = 1, 2$, $C = 0, N_e = \langle M * f_s/f_c \rangle$, $\zeta = \sqrt{2}Mf_s/f_c$, $\xi = 2N_e + 1$, ϵ.

1: Set $[\bar{\mathbf{Z}}_g]_{m,\mathcal{N}_e(n)} = 1$, if $[\tilde{Z}_g]_{m,n} > \epsilon$ & $[\tilde{Z}_g]_{m,n} > [\tilde{Z}_g]_{m,\,\mathrm{mod}\,(n+1)}$ & $[\tilde{Z}_g]_{m,n} > [\tilde{Z}_g]_{m,\,\mathrm{mod}\,(n-1)}$, where $[\tilde{Z}_g]_{m,n} \triangleq \frac{1}{T^u}\sum_{t=1}^{T^u} ||[\mathbf{Z}_g(t)]_{m,n}||_2$ and $\mathcal{N}_e(n) = \mathrm{mod}\,(n - N_e : n + N_e), g = 1, 2$;

2: $\mathbf{Z}_f = \bar{\mathbf{Z}}_1 \odot \bar{\mathbf{Z}}_2$;

3: $L_f = \sum_{m,n} [Z_f]_{m,n}$, $1 \le m \le M$, $1 \le n \le N$, $[\mathbf{I}_{\mathrm{dx}}]_{l,:} = [m_f(l), p_f(l)]$, where $(m_f(l), p_f(l))$ is the coordinate of the l-th nonzero element in $\mathbf{Z}_f$, $1 \le l \le L_f$;

4: $[\mathbf{D}]_{i,l} = (\min(|m_f(i) - m_f(l)|, |M + m_f(i) - m_f(l)|)^2 + \min(|p_f(i) - p_f(l)|, |N + p_f(i) - p_f(l)|)^2)^{1/2}$, $1 \le i, l \le L_f$;

5: **for** each unvisited support of $\mathbf{Z}_f$ **do**

6: mark the support as visited and set its index as l;

7: pick out $\mathcal{N}_b$ as $[\mathbf{D}]_{l,\mathcal{N}_b} < \zeta$. % find the support's neighborhood;

8: **if** $|\mathcal{N}_b| > \xi$ **then**

9: $C = C + 1$, mark the support as in the C-th cluster and set $k = 1$;

10: while 1

11: mark the k-th support in $|\mathcal{N}_b|$ as in the C-th cluster;

12: **if** the k-th support in $|\mathcal{N}_b|$ is unvisited **then**

13: mark the support as visited, pick out its neighborhood $\mathcal{N}_{bk}$ using **D** and threshold ζ;

14: $\mathcal{N}_b = [\mathcal{N}_b, \mathcal{N}_{bk}]$ if $|\mathcal{N}_{bk}| \ge \xi$;

15: **end if**

16: $k = k + 1$, quit the loop if $k > |\mathcal{N}_b|$;

17: **else**

18: mark the support as noise;

19: **end if**

20: **end for**

21: **return** the classified support matrix $\mathbf{L}_{idx}$ with its columns as angle domain index, delay domain index and the corresponding cluster number, respectively.

In Algorithm 2, step 2 transforms on-grid potential paths into off-grid ones. Step 3-5 are initialization steps. In step 3, φs; τs are selected angle, delay and measurement matrix in iterations, respectively. **R***it* is the residual of the *i*-th iteration in step 4. In step 5, S is the current sparsity level and *r* last is the residual of the last sparsity level. The MMV problem mentioned in (25) is solved in step 6-22. Step 7 to step 9 select a support that would most likely to be a true path under the current residual. Step 7 identifies the support that maximizes proxies of path gains and proxies of path gains are saved in **a***t* in step 8. Step 10-12 give an examination of supports under the current sparse level. Step 10 gives a least square (LS) estimation with the current φs (φs; τs). Support sets are reselected under the current sparse level in step 11 and a LS estimation under the current sparse level is given in step 12.

Algorithm 2 Proposed OSAMP Algorithm

Require: Received signal $\tilde{\mathbf{Y}}$, classified support matrix $\mathbf{L}_{idx}$ and threshold ς.

1: Update on-grid $\boldsymbol{\varphi}_0$ and $\boldsymbol{\tau}_0$ from supports of $\mathbf{L}_{idx}$ via (15), (16) and (19);
2: Update off-grid $\bar{\boldsymbol{\varphi}}$ and $\bar{\boldsymbol{\tau}}$ via (27) with $\boldsymbol{\varphi}_0$ and $\boldsymbol{\tau}_0$ as the initial point and $\tilde{\mathbf{Y}}$ as the residual until convergence meets, construct off-grid measurement matrix $\bar{\boldsymbol{\Phi}}(\bar{\boldsymbol{\varphi}}, \bar{\boldsymbol{\tau}})$ with $\bar{\boldsymbol{\varphi}}$ and $\bar{\boldsymbol{\tau}}$;
3: $\bar{\boldsymbol{\varphi}}_s = \bar{\boldsymbol{\tau}}_s = \bar{\boldsymbol{\Phi}}_s = \varnothing$;
4: $\mathbf{r}_t^0 = \tilde{\mathbf{Y}}_t \in \mathbb{C}^{MP\times 1}, \forall t$;
5: $\mathcal{S} = 1, r^{\text{last}} = +\infty$;
6: **repeat**
7: $\mathbf{a}_t = \left(\bar{\boldsymbol{\Phi}}(\bar{\boldsymbol{\varphi}}, \bar{\boldsymbol{\tau}})\right)_t^H \mathbf{r}_t^{j-1}, \forall t$;
8: $\mathcal{L}_{\max} = \arg\max_{\tilde{\mathcal{L}}_{\max}} \left\{\sum_{t=1}^{T^u} \left\|(\mathbf{a}_t)_{\tilde{\mathcal{L}}_{\max}}\right\|_2^2\right\}$;
9: Update $\bar{\boldsymbol{\varphi}}_s$, $\bar{\boldsymbol{\tau}}_s$ and $\bar{\boldsymbol{\Phi}}_s(\bar{\boldsymbol{\varphi}}_s, \bar{\boldsymbol{\tau}}_s)$ with the $\mathcal{L}_{\max}$-th support;
10: $\mathbf{b}_t = \left(\bar{\boldsymbol{\Phi}}_s(\bar{\boldsymbol{\varphi}}_s, \bar{\boldsymbol{\tau}}_s)\right)^\dagger \mathbf{r}_t, \forall t$;
11: $\Omega = \arg\max_{\tilde{\Omega}} \left\{\sum_{t=1}^{T^u} \left\|(\mathbf{b}_t)_{\tilde{\Omega}}\right\|_2^2, |\tilde{\Omega}| = \mathcal{S}\right\}$;
12: $\mathbf{c}_t = \left(\left(\bar{\boldsymbol{\Phi}}_s(\bar{\boldsymbol{\varphi}}_s, \bar{\boldsymbol{\tau}}_s)\right)_\Omega\right)^\dagger \mathbf{r}_t, \forall t$;
13: $\mathbf{r}_t = \tilde{\mathbf{Y}}_t - \left(\bar{\boldsymbol{\Phi}}_s(\bar{\boldsymbol{\varphi}}_s, \bar{\boldsymbol{\tau}}_s)\right)_\Omega \mathbf{c}_t, \forall t$;
14: $l_{\min} = \arg\min_{\tilde{l}} \left\{\sum_{t=1}^{T^u} \|[\mathbf{c}_t]_{\tilde{l}}\|_2^2, \tilde{l} \in \Omega\right\}$;
15: **if** $\sum_{t=1}^{T^u} \left\|[\mathbf{c}_t]_{l_{\min}}\right\|_2^2 / T^u \geq \varsigma$ and $\sum_{t=1}^{T^u} \|\mathbf{r}_t\|_2^2 \leq r^{\text{last}}$; **then**
16: **if** $\sum_{t=1}^{T^u} \|\mathbf{r}_t\|_2^2 \geq \sum_{t=1}^{T^u} \left\|\mathbf{r}_t^{i-1}\right\|_2^2$ **then**
17: $\mathcal{S} = \mathcal{S} + 1$, $r^{\text{last}} = \sum_{t=1}^{T^u} \left\|\mathbf{r}_t^{i-1}\right\|_2^2$ and $\mathbf{d}_t = \mathbf{c}_t$, record $\tilde{\boldsymbol{\varphi}}$, $\tilde{\boldsymbol{\tau}}$ and $\tilde{\boldsymbol{\Phi}}(\tilde{\boldsymbol{\varphi}}, \tilde{\boldsymbol{\tau}})$ with reselected set Ω;
18: **else**
19: update $\bar{\boldsymbol{\varphi}}_s$, $\bar{\boldsymbol{\tau}}_s$ and $\bar{\boldsymbol{\Phi}}_s(\bar{\boldsymbol{\varphi}}_s, \bar{\boldsymbol{\tau}}_s)$ with reselected set Ω and update residual $\mathbf{r}$;
20: **end if**
21: **end if**
22: **until** $\sum_{t=1}^{T^u} \left\|[\mathbf{c}_t]_{l_{\min}}\right\|_2^2 / T^u < \varsigma$ or $\sum_{t=1}^{T^u} \|\mathbf{r}_t\|_2^2 > r^{\text{last}}$.
23: Update off-grid $\tilde{\boldsymbol{\varphi}}_l$ and $\tilde{\boldsymbol{\tau}}_l$ via (27) with $\tilde{\boldsymbol{\varphi}}_l$ and $\tilde{\boldsymbol{\tau}}_l$ as the initial point and $\tilde{\mathbf{Y}} - \tilde{\boldsymbol{\Phi}}_{-l}(\tilde{\boldsymbol{\varphi}}, \tilde{\boldsymbol{\tau}})\mathbf{d}_{-l}$ as the residual until convergence meets, construct off-grid measurement matrix $\tilde{\boldsymbol{\Phi}}(\tilde{\boldsymbol{\varphi}}, \tilde{\boldsymbol{\tau}})$ with $\tilde{\boldsymbol{\varphi}}$ and $\tilde{\boldsymbol{\tau}}$.
24: **return** $\hat{\boldsymbol{\varphi}} = \tilde{\boldsymbol{\varphi}}$, $\hat{\boldsymbol{\tau}} = \tilde{\boldsymbol{\tau}}$ and $\hat{\mathbf{B}} = \left(\tilde{\boldsymbol{\Phi}}(\tilde{\boldsymbol{\varphi}}, \tilde{\boldsymbol{\tau}})\right)^\dagger \tilde{\mathbf{Y}}$.

The residual is updated in step 13. Step 14 finds the support of the minimum path gain amplitude according to **c***t*. Step 22 shows that if the minimal path gain is too small or the energy of residual of the current sparse level is larger than that of the last sparse level, the whole algorithm converges and no more iterations are needed. Thus step 15 gives the condition that the whole algorithm need more iterations to converge. Step 16 reveals that if the energy of residual of the current iteration is larger than that of the last iteration, the iteration of the current sparse level converges and a larger sparse level is encouraged while step 19 reveals that convergence is not met at the current sparse level. Step 23 makes up for the limitation of objective function. When V is used for the update of φ and τ, the inter-path interference exists and the channel estimation performance is limited. Thus we update φ and τ path by path and inter-path interference can be greatly reduced, which offers a good performance of our proposed algorithm.

Once φ, τ, β are obtained, the original uplink channel for all *N* subcarriers can be directly reconstructed as

$$\hat{\mathbf{H}}^u(t) = \sum_{l=1}^{\hat{L}} \hat{\beta}(l,t)[\mathbf{a}(\hat{\varphi}_l)\mathbf{b}^T(\hat{\tau}_l)] \odot \Theta(\hat{\varphi}_l).$$

DOWNLINK CHANNEL ESTIMATION

Downlink channel estimation is a challenging issue because it requires a huge demand of downlink pilots and feedback. Fortunately, if the difference between the uplink carrier frequency and the downlink carrier frequency is not large, i.e., $|fc - fd| << \min\{fc; fd\}$, where *fd* is the downlink carrier, the downlink angle and delay parameters would be the same to the uplink ones [35]. Such angle-delay reciprocity still holds for wideband channels [26] and it can be exploited for downlink channel estimation in FDD massive MIMO systems to reduce the overhead of downlink pilots and feedback.

For a certain time slot, the downlink channel on the *n*-th subcarrier can be written as

$$\mathbf{h}^d(n,t) = \sum_{l=1}^{L} \beta_l^d(t)\mathbf{a}\left(\left(1+\frac{(n-1)f_0}{f_d}\right)\varphi_l^d\right) e^{-j2\pi(n-1)f_0\tau_l^d},$$

where $\tau^d{}_l = \tau_l$ and the corresponding $\varphi^d{}_l$ can be expressed as

$$\varphi_l^d = \frac{d\sin\vartheta_l}{\lambda_d} = \frac{f_d}{f_c}\varphi_l,$$

where λd is the downlink transmission wavelength.

Note that the BS can acquire the DoA and delay information from the uplink channel extraction, which can be further utilized in downlink channel estimation at the BS side. Thus, we adopt a new CSI feedback and estimation framework that is introduced in [12] for downlink channel estimation. The procedure is shown as follows,

The BS sends pilots to the user side;

The user feeds the received signals back to the BS side without any signal processing. We here assume that the feedback is lossless;

The BS estimates the downlink path gains with the angle-delay information obtained from uplink training and reconstructs the downlink channel.

One advantage of the proposed framework is that all signal processing procedures are performed at the BS side, which simplifies requirements for signal processing at the user side. Moreover, random pilots can also work well in this framework. Assume that there are *Pd* subcarriers used for downlink pilot transmission, and the set of indexes of pilot subcarriers is denoted as P*d*. Denote **x***d* (*p*; *t*) 2 C*M*_1 as the downlink pilot on the *p*-th subcarrier. The received signal at the user side on the *p*-th subcarrier can be expressed as

$$y^d(p,t) = \sum_{l=1}^{L} (\beta_l^d(t))\mathbf{a}^T\left(\left(1+\frac{(\mathcal{P}_d(p)-1)f_0}{f_d}\right)\varphi_l^d\right) * e^{-j2\pi(\mathcal{P}_d(p)-1)f_0\tau_l^d}\mathbf{x}^d(p,t) + w_p^d.$$

RESULTS & DISCUSSION

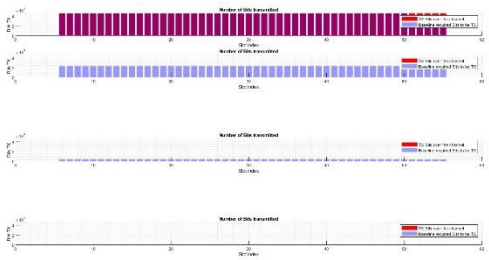

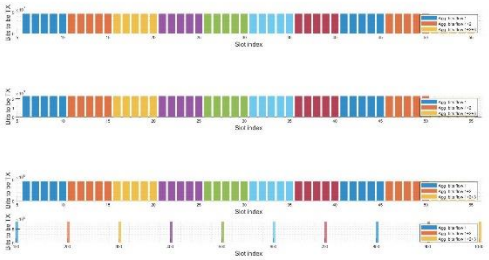

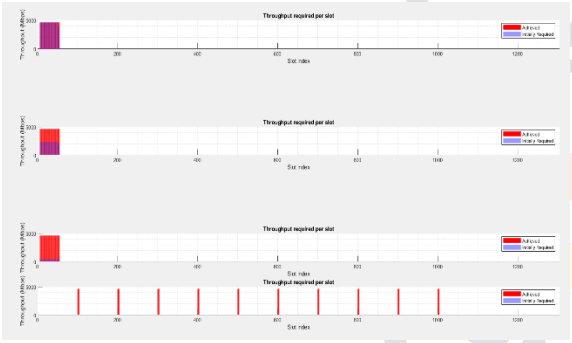

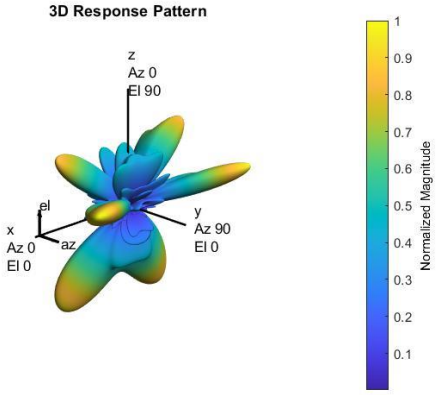

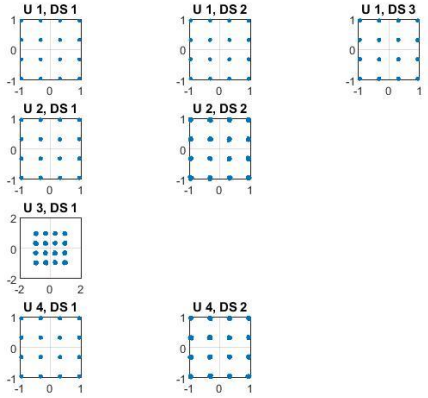


```
***** REPORT *****
ID=1
    OK=100.00(%)
    NOK=0.00(%)
ID=2
    OK=0.00(%)
    NOK=100.00(%)
ID=3
    OK=100.00(%)
    NOK=0.00(%)
ID=4
    OK=0.00(%)
    NOK=100.00(%)
ID=5
    OK=100.00(%)
    NOK=0.00(%)
ID=6
    OK=100.00(%)
    NOK=0.00(%)
Overall Performance: OK=66.67(%)
```

CONCLUSION

In this paper, we propose a low computational complexity channel extraction scheme for uplink and downlink channel estimation in wideband massive MIMO-OFDM systems, where the beam squint effect is considered. Firstly, we analyse the spatial- and frequency-wideband property of multi-subcarrier channels. Secondly, based on the multi-subcarrier channel property, we propose a pilot sub-carrier selection scheme by dividing pilot subcarriers into several groups in order to obtain a few qualified potential paths. Based on the uplink pilot signals received from different groups, we propose M-DBSCAN to extract potential paths. Thirdly, with the potential paths, we model the uplink channel extraction problem as a sparse signal reconstruction problem. Finally we propose OSAMP to estimate uplink channel parameters and reconstruct uplink channels. Effective downlink channel estimation scheme is also designed based on angle-delay reciprocity between uplink and down-link channels. Simulation results show that our proposed low-complexity schemes can achieve a similar performance with that of SBL in uplink channel estimation and outperform SBL in downlink channel estimation. Computational analysis indicates that our proposed low complexity algorithm is more suitable for systems with larger scale antennas and wider transmission bandwidth.

REFERENCES

[1] W. Ji, F. Zhang and L. Qiu, "Multipath Extraction Based UL/DL Channel Estimation for FDD Massive MIMO-OFDM Systems," in IEEE Access, vol. 9, pp. 75349-75361, 2021, doi: 10.1109/ACCESS.2021.3081497.

[2] E. G. Larsson, O. Edfors, F. Tufvesson, and T. L. Marzetta, ``Massive MIMO for next generation wireless systems," *IEEE Commun. Mag.*, vol. 52, no. 2, pp. 186_195, Feb. 2014.
[3] M. Agiwal, A. Roy, and N. Saxena, ``Next generation 5G wireless networks: A comprehensive survey," *IEEE Commun. Surveys Tuts.*, vol. 18, no. 3, pp. 1617_1655, 3rd Quart., 2016.
[4] T. L. Marzetta, ``Noncooperative cellular wireless with unlimited numbers of base station antennas," *IEEE Trans. Wireless Commun.*, vol. 9, no. 11, pp. 3590_3600, Nov. 2010.
[5] H. Q. Ngo, E. G. Larsson, and T. L. Marzetta, ``Energy and spectral efficiency of very large multiuser MIMO systems," *IEEE Trans. Commun.*, vol. 61, no. 4, pp. 1436_1449, Apr. 2013.
[6] H. Xie, F. Gao, S. Zhang, and S. Jin, ``A unified transmission strategy for TDD/FDD massive MIMO systems with spatial basis expansion model," *IEEE Trans. Veh. Technol.*, vol. 66, no. 4, pp. 3170_3184, Apr. 2017.
[7] B. Halvarsson, A. Simonsson, A. Elgcrona, R. Chana, P. Machado, and H. Asplund, ``5G NR testbed 3.5 GHz coverage results," in *Proc. IEEE 87th Veh. Technol. Conf. (VTC Spring)*, Jun. 2018, pp. 1_5.
[8] O. E. Ayach, S. Rajagopal, S. Abu-Surra, Z. Pi, and R. W. Heath, Jr., ``Spatially sparse precoding in millimeter wave MIMO systems," *IEEE Trans. Wireless Commun.*, vol. 13, no. 3, pp. 1499_1513, Mar. 2014.
[9] A. A. Esswie and K. I. Pedersen, ``Opportunistic spatial preemptive scheduling for URLLC and eMBB coexistence in multi-user 5G networks," *IEEE Access*, vol. 6, pp. 38451_38463, Jul. 2018.
[10] H. Yin, L. Zhang, and S. Roy, ``Multiplexing URLLC traffic within Embb services in 5G NR: Fair scheduling," *IEEE Trans. Commun.*, vol. 69, no. 2, pp. 1080_1093, Feb. 2021.
[11] J. Choi, Z. Chance, D. J. Love, and U. Madhow, ``Noncoherent trellis coded quantization: A practical limited feedback technique for massive MIMO systems," *IEEE Trans. Commun.*, vol. 61, no. 12, pp. 5016_5029, Dec. 2013.
[12] W. Shen, L. Dai, B. Shim, Z. Wang, and R. W. Heath, Jr., ``Channel feedback based on AoD-adaptive subspace codebook in FDD massive MIMO systems," *IEEE Trans. Commun.*, vol. 66, no. 11, pp. 5235_5248, Nov. 2018.
[13] X. Rao and V. K. N. Lau, ``Distributed compressive CSIT estimation and feedback for FDD multi-user massive MIMO systems," *IEEE Trans. Signal Process.*, vol. 62, no. 12, pp. 3261_3271, May 2014.
[14] K. Xu, X. Xia, Y. Wang, and X. Yang, ``Channel acquisition for hybrid analog-digital mMIMO system by exploiting the clustered sparsity," in *Proc. IEEE Int. Conf. Commun. (ICC)*, May 2019, pp. 1_6.
[15] X. Xia, K. Xu, S. Zhao, and Y.Wang, ``Learning the time-varying massive MIMO channels: Robust estimation and data-aided prediction," *IEEE Trans. Veh. Technol.*, vol. 69, no. 8, pp. 8080_8096, Aug. 2020.
[16] K. Xu, Z. Shen, Y. Wang, and X. Xia, ``Location-aided mMIMO channel tracking and hybrid beamforming for high-speed railway communications: An angle-domain approach," *IEEE Syst. J.*, vol. 14, no. 1, pp. 93_104, Mar. 2020.
[17] C. Tseng, J. Wu, and T. Lee, ``Enhanced compressive downlink CSI recovery for FDD massive MIMO systems using weighted block `1-minimization," *IEEE Trans. Commun.*, vol. 64, no. 3, pp. 1055_1067, Jan. 2016.
[18] W. Shen, L. Dai, Y. Shi, B. Shim, and Z.Wang, ``Joint channel training and feedback for FDD massive MIMO systems," *IEEE Trans. Veh. Technol.*, vol. 65, no. 10, pp. 8762_8767, Oct. 2016.
[19] X. Cheng, J. Sun, and S. Li, ``Channel estimation for FDD multi-user massive MIMO: A variational Bayesian inference-based approach," *IEEE Trans. Wireless Commun.*, vol. 16, no. 11, pp. 7590_7602, Nov. 2017.
[20] A. Liu, L. Lian, V. K. N. Lau, and X. Yuan, ``Downlink channel estimation in multiuser massive MIMO with hidden Markovian sparsity," *IEEE Trans. Signal Process.*, vol. 66, no. 18, pp. 4796_4810, Sep. 2018.
[21] Z. Gao, L. Dai, Z. Wang, and S. Chen, ``Spatially common sparsity based adaptive channel estimation and feedback for FDD massive MIMO," *IEEE Trans. Signal Process.*, vol. 63, no. 23, pp. 6169_6183, Dec. 2015.
[22] P.-H. Kuo, H. T. Kung, and P.-A. Ting, ``Compressive sensing-based channel feedback protocols for spatially-correlated massive antenna arrays," in *Proc. IEEE Wireless Commun. Netw. Conf. (WCNC)*, Apr. 2012, pp. 492_497.
[23] X.-L. Huang, J. Wu, Y. Wen, F. Hu, Y. Wang, and T. Jiang, ``Rate-adaptive feedback with Bayesian compressive sensing in multiuser MIMO beamforming systems," *IEEE Trans. Wireless Commun.*, vol. 15, no. 7, pp. 4839_4851, Jul. 2016.
[24] J. Dai, A. Liu, and V. K. N. Lau, ``FDD massive MIMO channel estimation with arbitrary 2D-array geometry," *IEEE Trans. Signal Process.*, vol. 66, no. 10, pp. 2584_2599, May 2018.
[25] J. Dai, A. Liu, and V. K. N. Lau, ``Joint channel estimation and user grouping for massive MIMO systems," *IEEE Trans. Signal Process.*, vol. 67, no. 3, pp. 622_637, Feb. 2019.
[26] H. Tang, J. Wang, and L. He, ``Off-grid sparse Bayesian learning-based channel estimation for mmWave massive MIMO uplink," *IEEE Wireless Commun. Lett.*, vol. 8, no. 1, pp. 45_48, Feb. 2019.
[27] B. Wang, F. Gao, S. Jin, H. Lin, and G. Y. Li, ``Spatial- and frequency-wideband effects in millimeter-wave massive MIMO systems," *IEEE Trans. Signal Process.*, vol. 66, no. 13, pp. 3393_3406, Jul. 2018.
[28] U. Ugurlu, R. Wichman, C. B. Ribeiro, and C. Wijting, ``A multipath extraction-based CSI acquisition method for FDD cellular networks with massive antenna arrays," *IEEE Trans. Wireless Commun.*, vol. 15, no. 4, pp. 2940_2953, Apr. 2016.
[29] L. You, X. Gao, A. L. Swindlehurst, and W. Zhong, ``Channel acquisition for massive MIMO-OFDM with adjustable phase shift pilots," *IEEE Trans. Signal Process.*, vol. 64, no. 6, pp. 1461_1476, Mar. 2016.
[30] M. Jian, F. Gao, Z. Tian, S. Jin, and S. Ma, ``Angle-domain aided UL/DL channel estimation for wideband mmWave massive MIMO systems with beam squint," *IEEE Trans. Wireless Commun.*, vol. 18, no. 7, pp. 3515_3527, Jul. 2019.
[31] B. Wang, M. Jian, F. Gao, G. Y. Li, and H. Lin, ``Beam squint and channel estimation for wideband mmWave massive MIMO-OFDM systems," *IEEE Trans. Signal Process.*, vol. 67, no. 23, pp. 5893_5908, Dec. 2019.
[32] M.Wang, F. Gao, N. Shlezinger, M. F. Flanagan, and Y. C. Eldar, ``A block sparsity based estimator for mmWave massive MIMO channels with beam squint," *IEEE Trans. Signal Process.*, vol. 68, pp. 49_64, Nov. 2020.
[33] J. Fang, F. Wang, Y. Shen, H. Li, and R. S. Blum, ``Super-resolution compressed sensing for line spectral estimation: An iterative reweighted approach," *IEEE Trans. Signal Process.*, vol. 64, no. 18, pp. 4649_4662, Sep. 2016.
[34] D. Tse and P. Viswanath, *Fundamentals of Wireless Communication*. Cambridge, U.K.: Cambridge Univ. Press, 2004.

[35] T. L. Hansen, M. A. Badiu, B. H. Fleury, and B. D. Rao, ``A sparse Bayesian learning algorithm with dictionary parameter estimation," in *Proc. IEEE 8th Sensor Array Multichannel Signal Process. Workshop (SAM)*, Jun. 2014, pp. 385_388.

[36] G. G. Raleigh, S. N. Diggavi, V. K. Jones, and A. Paulraj, ``A blind adaptive transmit antenna algorithm for wireless communication," in *Proc. IEEE Int. Conf. Commun. (ICC)*, Jun. 1995, pp. 1494_1499.